Contents lists available at ScienceDirect

# Nuclear Inst. and Methods in Physics Research, A

# Measurement of the electron–hole pair creation energy in $Al_{0.52}In_{0.48}P$ using X-ray radiation

CrossMark

S. Butera [a],*, G. Lioliou [a], A.B. Krysa [b], A.M. Barnett [a]

[a] Space Research Group, School of Engineering and Informatics, University of Sussex, Brighton, BN1 9QT, UK
[b] EPSRC National Centre for III-V Technologies, University of Sheffield, Mappin Street, Sheffield, S1 3JD, UK

ABSTRACT

The average energy consumed in the generation of an electron–hole pair ($\varepsilon_{AlInP}$) in $Al_{0.52}In_{0.48}P$ was experimentally measured across the temperature range −20 °C to 100 °C, using a custom AlInP X-ray-photodiode, an $^{55}Fe$ radioisotope X-ray source, and custom low-noise charge-sensitive preamplifier electronics. $\varepsilon_{AlInP}$ was found to linearly decrease with increasing temperature according to the equation $\varepsilon_{AlInP}$ = (-0.0033 eV/K ± 0.0003 eV/K)$T$ + (6.31 eV ± 0.10 eV). At room temperature (20 °C), $\varepsilon_{AlInP}$ = 5.34 eV ± 0.07 eV.

## 1. Introduction

Photon counting X-ray spectrometers that can operate in harsh environments (high temperature, intense radiation) are increasingly important for extreme terrestrial and space exploration applications. Wide bandgap semiconductors, such as GaAs [1,2], AlGaAs [3], and SiC [4], have been investigated as detector materials for such X-ray spectrometers. Compared to narrower bandgap semiconductors, such as Si, wide bandgap materials have the advantage of being able to operate at elevated temperatures without cooling systems due to their smaller thermally generated currents.

Recently, $Al_{0.52}In_{0.48}P$ photon counting X-ray spectrometers have been demonstrated for the first time in non-avalanche [5] and avalanche [6] modes. $Al_{0.52}In_{0.48}P$ has an indirect bandgap of 2.31 eV [7]; $Al_xIn_{1-x}P$ with different Al fractions correspond to different bandgaps: in principle, the Al fraction can vary from 0, corresponding to a bandgap of 2.5 eV (in this case it reduces to the binary compound InP), to 1, corresponding to a bandgap of 1.34 eV (in this case it reduces to the binary compound AlP). Due to its bandgap, $Al_{0.52}In_{0.48}P$ devices present low thermally generated leakage currents even at high temperatures [5,8]. $Al_{0.52}In_{0.48}P$ has a high effective atomic number, and hence relatively high linear X-ray attenuation coefficient, as a consequence of the presence of Indium (atomic number 49) [9]. This results in higher X-ray quantum efficiency per unit thickness [5] compared to some other wide bandgap X-ray photodetectors, e.g. SiC, AlGaAs, and GaAs [10,11]. $Al_{0.52}In_{0.48}P$ is nearly lattice matched with commercially available GaAs substrates and can be grown with high crystalline

quality. The ability to more easily control the doping in $Al_{0.52}In_{0.48}P$ with respect to some II–VI semiconductors [12] is also beneficial. All these characteristics make $Al_{0.52}In_{0.48}P$ highly promising for future X-ray and $\gamma$-ray detectors. Although $Al_{0.52}In_{0.48}P$ has received significant research attention at optical wavelengths, e.g. as a barrier material in quantum well structures [13,14], cladding layers in laser diodes [15,16], optical windows in solar cells [17], blue–green optical detectors [7,18] etc., many material properties have not yet been reported; this is particularly true for properties related to the compound's use in X-ray, $\gamma$-ray, and charged particle detection. Measurements of the average energy consumed in the generation of an electron–hole pair ($\varepsilon_{AlInP}$) and the Fano factor ($F$), for example, have not yet been reported, despite the knowledge of $\varepsilon_{AlInP}$ and $F$ being important since they determine the statistically limited energy resolution of an X-ray detector [19].

The fundamental statistically limited energy resolution in terms of Full Width at Half Maximum (FWHM, in eV) of a non-avalanche semiconductor detector is given by:

$$FWHM[eV] = 2.35\varepsilon\sqrt{\frac{FE}{\varepsilon}} \tag{1}$$

where $\varepsilon$ is the semiconductor's electron–hole pair creation energy, $F$ is the semiconductor's Fano factor, and $E$ is the X-ray photon's energy.

It must be underlined that the energy consumed in the generation of an electron–hole pair at X-ray energies in a semiconductor differs from its bandgap; whilst the $Al_{0.52}In_{0.48}P$ bandgap is well known [7], until now there have been no experimental measurements of $\varepsilon_{AlInP}$.

---

* Corresponding author.
E-mail address: S.Butera@sussex.ac.uk (S. Butera).

**Table 1**

Layer details of the $Al_{0.52}In_{0.48}P$ X-ray photodiode.

| Layer | Material | Thickness (μm) | Dopant | Dopant type | Doping density (cm$^{-3}$) |
|---|---|---|---|---|---|
| 1 | Ti | 0.02 | | | |
| 2 | Au | 0.2 | | | |
| 3 | GaAs | 0.01 | Zn | P$^+$ | $1 \times 10^{19}$ |
| 4 | $Al_{0.52}In_{0.48}P$ | 0.2 | Zn | P$^+$ | $5 \times 10^{17}$ |
| 5 | $Al_{0.52}In_{0.48}P$ | 2 | Undoped | | |
| 6 | $Al_{0.52}In_{0.48}P$ | 0.1 | Si | n$^+$ | $2 \times 10^{18}$ |
| 7 | Substrate n$^+$ GaAs | | | | |
| 8 | InGe | 0.02 | | | |
| 9 | Au | 0.2 | | | |

**Table 2**

Layer details of the GaAs X-ray photodiode.

| Layer | Material | Thickness (μm) | Dopant | Dopant type | Doping density (cm$^{-3}$) |
|---|---|---|---|---|---|
| 1 | Ti | 0.02 | | | |
| 2 | Au | 0.2 | | | |
| 3 | GaAs | 0.5 | Be | P$^+$ | $2 \times 10^{18}$ |
| 4 | GaAs | 10 | Undoped | | $<10^{15}$ |
| 5 | GaAs | 1 | Si | n$^+$ | $2 \times 10^{18}$ |
| 6 | Substrate n$^+$ GaAs | | | | |
| 7 | InGe | 0.02 | | | |
| 8 | Au | 0.2 | | | |
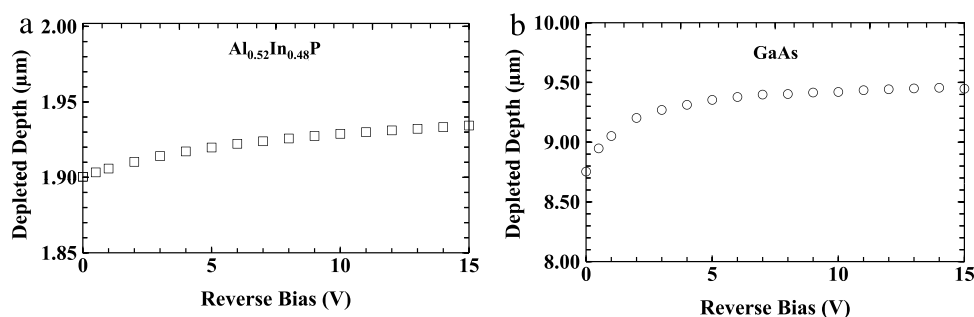


**Fig. 1.** Depletion depth as a function of applied reverse bias at room temperature (a) for the $Al_{0.52}In_{0.48}P$ device (empty squares), and (b) for the GaAs devices (empty circles).

## 2. Results

Firstly, the average energy consumed in the generation of an electron–hole pair (commonly called the electron–hole pair creation energy) in $Al_{0.52}In_{0.48}P$ ($\varepsilon_{AlInP}$) was measured at room temperature (20 °C), using a custom $Al_{0.52}In_{0.48}P$ X-ray photodiode, an $^{55}$Fe radioisotope X-ray source, custom low-noise charge-sensitive preamplifier electronics, and a high-purity reference GaAs X-ray photodiode. The method used was similar to that used by other researchers to determine the electron–hole pair creation energies for GaAs, SiC, $Al_{0.8}Ga_{0.2}As$, and $Al_{0.2}Ga_{0.8}As$ [20–23]: the electron–hole pair creation energy for $Al_{0.52}In_{0.48}P$ was experimentally determined by measuring the amount of charge created by the absorption of X-rays from an $^{55}$Fe radioisotope X-ray source (Mn K$\alpha$: 5.9 keV; Mn K$\beta$: 6.49 keV) in the $Al_{0.52}In_{0.48}P$ photodiode relative to that created in GaAs [20–23].

A 200 μm diameter mesa $Al_{0.52}In_{0.48}P$ photodiode was grown by metalorganic vapour phase epitaxy (MOVPE) on a (100) n-GaAs: Si substrate with a misorientation of 10 degrees towards ⟨111⟩A to suppress the CuPt-like ordered phase [24]. The $Al_{0.52}In_{0.48}P$ structure is summarised in Table 1. Preliminarily characterisation of the $Al_{0.52}In_{0.48}P$ photodiode was performed to ensure its suitability for the measurements [5]. A well characterised high-purity 200 μm diameter mesa GaAs photodiode [25] was used as the GaAs reference detector; the structure of which is summarised in Table 2. It has to be noted that both the $Al_{0.52}In_{0.48}P$ and the GaAs devices were P–i–n structures.

The $Al_{0.52}In_{0.48}P$ photodiode was connected in parallel with the GaAs reference detector, to a custom-made low-noise charge-sensitive preamplifier of feedback resistorless design, similar to Ref. [26]. The output of the preamplifier was connected to an Ortec 572a shaping amplifier

and then to a multichannel analyser (MCA). An $^{55}$Fe radioisotope X-ray source was positioned, in turn, above of each of the $Al_{0.52}In_{0.48}P$ and GaAs mesa photodiodes (5 mm away from the photodiodes' surface in each case). Measurements were taken at room temperature when both detectors were reverse biased at 10 V (electric field strength across the $Al_{0.52}In_{0.48}P$ detector of 50 kV/cm): preliminary results had shown that both the $Al_{0.52}In_{0.48}P$ and GaAs detectors were fully depleted at 10 V (Figs. 1 and 2 report the calculated depletion region and the expected carrier concentrations for both the $Al_{0.52}In_{0.48}P$ [5] and the GaAs detectors [25]), and exhibited negligible charge trapping in this bias condition. Spectra were accumulated with the $^{55}$Fe radioisotope X-ray source illuminating the $Al_{0.52}In_{0.48}P$ and GaAs devices in turn. The X-ray photopeaks were each the combination of the Mn K$\alpha$ and Mn K$\beta$ lines from the $^{55}$Fe radioisotope X-ray source. Gaussians were fitted to the photopeak obtained with each detector taking into account the relative X-ray emission rates of the $^{55}$Fe radioisotope X-ray source [27] and the relative differences in efficiency of the detectors at these X-ray energies. Energy resolutions (FWHM) at 5.9 keV of 1.32 keV and 1.09 keV were measured when the $^{55}$Fe radioisotope X-ray source was illuminating the $Al_{0.52}In_{0.48}P$ and the GaAs devices, respectively. These values were larger than those measured when the detectors were individually connected to the preamplifier i.e. 960 eV FWHM at 5.9 keV with the $Al_{0.52}In_{0.48}P$ detector [5] and 660 eV FWHM at 5.9 keV with the GaAs detector [25] both at room temperature. Broadened energy resolutions were observed in the present case because the $Al_{0.52}In_{0.48}P$ and the GaAs photodiodes were connected in parallel with each other to the preamplifier. The detector capacitances (2.4 pF for the $Al_{0.52}In_{0.48}P$ detector, and 1.10 pF for the GaAs detector) and leakage currents (0.19 pA for the $Al_{0.52}In_{0.48}P$ detector, and 4.4 pA for the GaAs detector) summed, resulting in

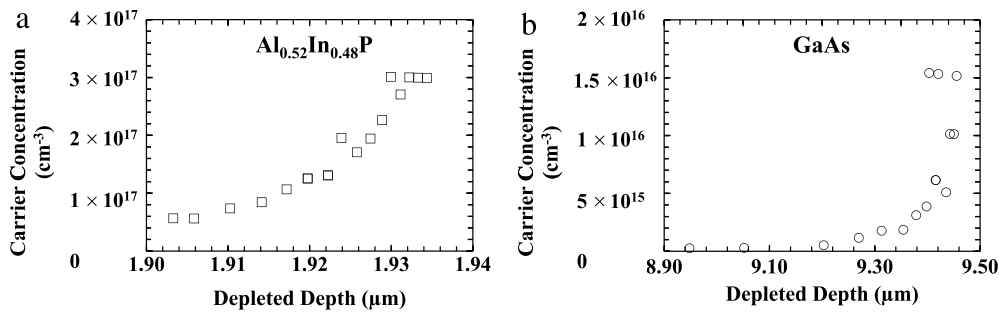**Fig. 2.** Doping concentration below the P$^+$-i junction as a function of depletion depth at room temperature (a) for the Al$_{0.52}$In$_{0.48}$P device, and (b) for the GaAs device.
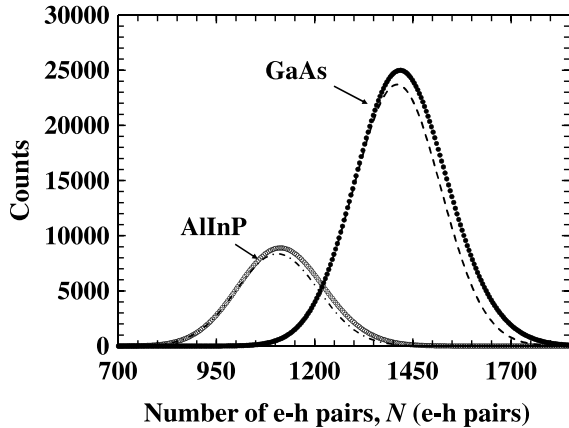


**Fig. 3.** $^{55}$Fe X-ray spectra accumulated at 10 V reverse bias and at room temperature (20 °C), using the Al$_{0.52}$In$_{0.48}$P device (empty circles) and the GaAs reference photodetector (filled circles). Also shown are the fitted 5.9 keV peaks for the Al$_{0.52}$In$_{0.48}$P device (dashed-dot line) and the GaAs reference photodetector (dashed line).

increased series white noise and parallel white noise; thus, leading to the observed FWHM broadening.

Fig. 3 shows the $^{55}$Fe X-ray spectra accumulated with the Al$_{0.52}$In$_{0.48}$P device and the GaAs reference photodetector together with the Gaussians fitted to represent the Mn K$\alpha$ (5.9 keV) photopeaks deconvolved from the combined Mn K$\alpha$ and K$\beta$ emissions from the source in each case. The spectra were plotted as a function of charge (in units of electron–hole pairs generated) where the MCA scale was charge calibrated based on the positions of the zero energy noise peak of the preamplifier in this configuration and the 5.9 keV Mn K$\alpha$ photopeak detected by GaAs reference photodetector, given the accepted value of the electron–hole pair creation energy in GaAs (4.184 eV $\pm$ 0.025 eV) [20].

As evident from Fig. 3, the average number of electron–hole pairs created by the absorption of a photon of energy $E$ in the GaAs reference detector ($N_{GaAs}$) is greater than that created in Al$_{0.52}$In$_{0.48}$P ($N_{AlInP}$), this is a consequence of the larger electron–hole pair creation energy in Al$_{0.52}$In$_{0.48}$P ($\varepsilon_{AlInP}$) compared with GaAs ($\varepsilon_{GaAs}$). Assuming trapping and recombination processes are negligible (i.e. charge collection efficiencies = 1 in both cases [5,25]), the electron–hole pair creation energy in Al$_{0.52}$In$_{0.48}$P was determined knowing $\varepsilon_{GaAs}$ and the measured ratio ($N_{GaAs}/N_{AlInP}$), according Eq. (2) [22,23]:

$$\varepsilon_{AlInP} = \varepsilon_{GaAs} \left( \frac{N_{GaAs}}{N_{AlInP}} \right). \tag{2}$$

It was found that $\varepsilon_{AlInP} = 5.34$ eV $\pm$ 0.07 eV at 20 °C.

The assumption of complete charge collection efficiency was adopted following preliminary investigation of both detectors which showed no evidence of incomplete charge collection [5,25]. Furthermore, it has been experimentally demonstrated that epitaxial GaAs layers have mean

drift lengths of charge carriers as high as 1.5 mm at 50 kV/cm electric fields [28], thus further reinforcing this assumption for the 10 μm thick GaAs reference detector.

However, to further ensure that the assumption of complete charge collection in the Al$_{0.52}$In$_{0.48}$P detector was valid, the experiment was repeated with increased electric field strength (reverse bias) across the Al$_{0.52}$In$_{0.48}$P detector; field strengths of 75 kV/cm (15 V) and 100 kV/cm (20 V) were investigated and further confirmed the negligibility of any charge trapping effects; had a significant reduction in apparent electron–hole pair creation energy been obtained from such measurements it would have suggested the presence of improved charge collection at these higher field strengths, thus suggesting incomplete collection at 50 kV/cm (10 V), however no such reduction was observed. $\varepsilon_{AlInP}$ values of 5.35 eV $\pm$ 0.07 eV and 5.36 eV $\pm$ 0.07 eV were obtained at 15 V and 20 V, respectively. Since an error of $\pm$0.07 eV was associated with $\varepsilon_{AlInP}$, the variation in the electron–hole pair creation energy measured at different voltages was negligible.

The Al$_{0.52}$In$_{0.48}$P electron–hole pair creation energy was then studied across the temperature range −20 °C to 100 °C. The GaAs reference photodetector was removed from the experimental spectrometer setup; the Al$_{0.52}$In$_{0.48}$P device was individually connected to the custom-made low-noise charge-sensitive preamplifier. The $^{55}$Fe radioisotope X-ray source, the Al$_{0.52}$In$_{0.48}$P device, and the custom low noise charge-sensitive preamplifier were placed inside a TAS Micro MT climatic cabinet for temperature control. A stabilised pulse generator (Berkeley Nucleonics Corporation model BH-1) was connected to the test signal input of the custom preamplifier such that the change in conversion factor of the preamplifier itself with temperature could be measured and its effects taken into account in the subsequent analysis [23,29]. The changes in the test capacitance of the preamplifier with temperature were also appropriately taken into account. Spectra were collected at each temperature studied. At each temperature, the photopeak and the peak from the pulse generator were analysed, Gaussians were fitted to them (taking account of the Mn K$\alpha$ and Mn K$\beta$ peaks in the case of the photopeak), and the position of their centroids with respect to the zero noise peak were computed. The relative change in position of the photopeak's Mn K$\alpha$ peak on the MCA's charge scale when corrected for the preamplifier's change in conversion factor with temperature (as determined from the pulser peak) gave information about the relative change in the charge created in the Al$_{0.52}$In$_{0.48}$P device by the photons from $^{55}$Fe radioisotope X-ray source at different temperatures [23,29]. This change was caused by the change of the Al$_{0.52}$In$_{0.48}$P electron–hole pair creation energy with temperature [23,29]. Knowing the electron–hole pair creation energy at 20 °C (5.34 eV $\pm$ 0.07 eV), it was possible to calculate the absolute value of the electron–hole pair creation energy at each temperature studied. Fig. 4 shows the Al$_{0.52}$In$_{0.48}$P electron–hole pair creation energy as a function of temperature.

The average energy consumed in the production of an electron–hole pair in Al$_{0.52}$In$_{0.48}$P decreased at increased temperature; a value of 5.48 eV $\pm$ 0.08 eV was recorded at −20 °C, which decreased to 5.04 eV $\pm$ 0.07 eV at 100 °C (96% of the value at −20 °C). A linear relationship between the Al$_{0.52}$In$_{0.48}$P electron–hole pair creation energy and temperature

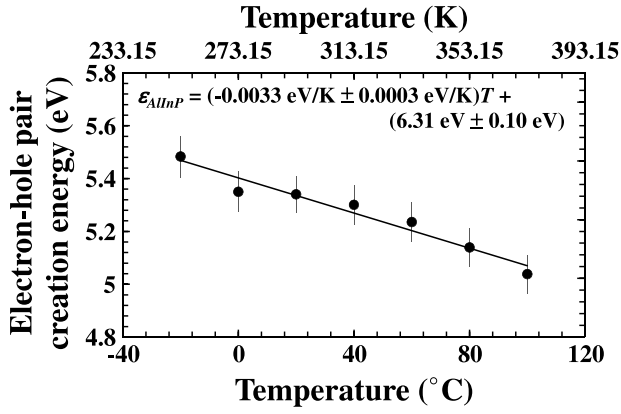**Fig. 4.** Temperature dependence of the energy consumed to produce an electron–hole pair in $Al_{0.52}In_{0.48}P$.



**Fig. 5.** Electron–hole pair creation energy for Ge, Si, GaAs, $Al_{0.2}Ga_{0.8}As$, $Al_{0.8}Ga_{0.2}As$, and $Al_{0.52}In_{0.48}P$ as a function of their bandgap energy at 300 K.

was observed; comparison of the standard deviation of the fitting with the experimental uncertainties demonstrated that the linear fitting was appropriate within the uncertainties of the experiment. Fig. 4 shows the linear least square fit that was performed on the data: $\varepsilon_{AlInP} = A\,T + B$ with $A = (-0.0033 \pm 0.0003)$ eV/K, $B = (6.31 \pm 0.10)$ eV. The gradient of the line of the best fit, representing the temperature dependence of the $Al_{0.52}In_{0.48}P$ electron–hole pair creation energy, was steeper than that reported for GaAs ($-0.00122$ eV/K [20]) but shallower than that reported for $Al_{0.8}Ga_{0.2}As$ ($-0.0077$ eV/K [29]). The gradient was similar to that reported for $Al_{0.2}Ga_{0.8}As$ ($-0.003$ eV/K [23]).

Assuming a temperature independent Fano factor of 0.12 (the Fano factor for $Al_{0.52}In_{0.48}P$ has not been reported yet; a value of 0.12 was assumed based on measurements of the parameter in other wide bandgap materials such as GaAs [30]), it was possible to estimate the statistically limited (i.e. "Fano limited") energy resolution for $Al_{0.52}In_{0.48}P$ detectors using Eq. (1) and the now determined electron–hole pair creation energy at different temperatures: FWHM at 5.9 keV of 140 eV and 146 eV were calculated for temperatures of 100 °C and −20 °C, respectively. It should be noted that measurements of the Fano factor as a function of temperature are yet to be reported for $Al_{0.52}In_{0.48}P$, so these values for the statistically limited energy resolution should be considered provisional.

The dependence of the electron–hole pair creation energy on semiconductor physical parameters has received much study in the past using a variety of incident radiation types [31]. Many researchers agreed on some dependence of $\varepsilon$ on bandgap energy [32–34]. According Klein [34], the empirical relationship between the electron–hole pair creation energy and the bandgap energy in a semiconductor is given by:

$$\varepsilon = \left(\frac{14}{5}\right) E_g + r\,(\hbar\omega) \tag{3}$$

where $E_g$ is the semiconductor bandgap, and $r\,(\hbar\omega)$ is the contribution due optical phonon losses ($r$ is the average number of optical phonons of energy $\hbar\omega$). Owens and Peacock [35] reported that, although many materials almost fit the Klein description in Eq. (3) when $r\,(\hbar\omega) = 0.6$ eV [34,35] (the "main Klein function branch"), a number of materials including $HgI_2$, $PbI_2$, TlBr, diamond, and AlN are displaced to lower values which led to the suggestion that there was a secondary Klein function branch with $r\,(\hbar\omega) = -1.5$ eV [35]. However, it is generally recognised that $r\,(\hbar\omega) < 0$ in Eq. (3) is unphysical, and therefore the Klein function explanation for the relationship between the bandgap energy and the electron–hole pair creation energy is unsatisfactory as noted by Owens and Peacock [35]. Questions have also been raised about the validity of the Klein plots due to the differing temperatures at which the materials were measured and the dubious quality of some included materials [29]. A further problem exists because $Al_{0.8}Ga_{0.2}As$ and $Al_{0.2}Ga_{0.8}As$ fit neither the main nor secondary Klein branches [22,23]. This latter problem

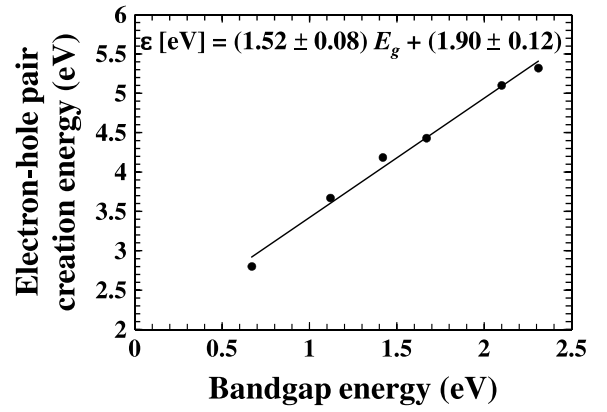led to the identification of the empirical Bertuccio–Maiocchi–Barnett (BMB) relationship [23] which plots the electron–hole pair creation energy as a function of bandgap energy both at a temperature of 300 K only including values determined from materials known to be of high quality, namely Ge, Si, GaAs, $Al_{0.2}Ga_{0.8}As$, and $Al_{0.8}Ga_{0.2}As$. The BMB relationship [23] suggests that at 300 K,

$$\varepsilon\,[\text{eV}] = (1.58 \pm 0.09)\,E_g + (1.83 \pm 0.13). \tag{4}$$

Like $Al_{0.8}Ga_{0.2}As$ and $Al_{0.2}Ga_{0.8}As$, the electron–hole pair creation energy estimated for $Al_{0.52}In_{0.48}P$ at 300 K (5.32 eV ± 0.10 eV) fits neither the main nor secondary Klein functions. If $Al_{0.52}In_{0.48}P$ lay on the main Klein branch a value of 7.07 eV would have been obtained. If $Al_{0.52}In_{0.48}P$ lay on the secondary Klein branch a value of 4.94 eV would have been obtained. However, the value obtained for $Al_{0.52}In_{0.48}P$ is in agreement with the BMB relationship which suggests a value of 5.48 eV ± 0.25 eV.

In Fig. 5, the BMB relationship is plotted and refined using the electron–hole pair creation energy for $Al_{0.52}In_{0.48}P$ at 300 K as estimated in this article. A linear least squares fit of the data including $Al_{0.52}In_{0.48}P$ shows that the BMB relationship can be refined to be

$$\varepsilon\,[\text{eV}] = (1.52 \pm 0.08)\,E_g + (1.90 \pm 0.12). \tag{5}$$

The equations for the BMB relationship as described in Eqs. (4) and (5) agree within their uncertainties, and the new data for $Al_{0.52}In_{0.48}P$ has enabled a modest reduction in the associated uncertainties.

## 3. Conclusion

In conclusion, the average energy consumed in the generation of an electron–hole pair in $Al_{0.52}In_{0.48}P$ ($\varepsilon_{AlInP}$) has been experimentally measured. By measuring the charge created in $Al_{0.52}In_{0.48}P$ from the absorption of X-ray photons emitted by an $^{55}Fe$ radioisotope X-ray source (Mn K$\alpha$ = 5.9 keV, Mn K$\beta$ = 6.49 keV) a value of 5.34 eV ± 0.07 eV for $\varepsilon_{AlInP}$ was measured at room temperature (20 °C). The results show that $Al_{0.52}In_{0.48}P$ is another material which does not fit either branch of the Klein function relating electron–hole pair creation energy and bandgap energy. However, the obtained value at 300 K is in agreement with that predicted by the Bertuccio–Maiocchi–Barnett (BMB) relationship. Using the new data for $Al_{0.52}In_{0.48}P$, the BMB relationship can be refined such that it becomes $\varepsilon\,[\text{eV}] = (1.52 \pm 0.08)E_g + (1.90 \pm 0.12)$. This is in agreement with the previous values identified in the BMB relationship but the uncertainties have been reduced. The temperature dependence of the electron–hole pair creation energy in $Al_{0.52}In_{0.48}P$ was measured across the range −20 °C to 100 °C. It was found to linearly decrease from 5.48 eV ± 0.08 eV at −20 °C to 5.04 eV ± 0.07 eV at 100 °C with $\varepsilon_{AlInP} = AT + B$ where $A = (-0.0033 \pm 0.0003)$ eV/K, and $B = (6.31 \pm 0.10)$ eV.

## Acknowledgements

Data underlying this work are subject to commercially confidentiality. The Authors regret that they cannot grant public requests for further access to any data produced during the study.

## References

[1] G. Lioliou, X. Meng, J.S. Ng, A.M. Barnett, J. Appl. Phys. 119 (2016) 124507.
[2] A. Owens, M. Bavdaz, A. Peacock, A. Poelaert, H. Andersson, S. Nenonen, L. Troger, G. Bertuccio, Nucl. Instrum. Methods. Phys. Res. Sect. A 466 (2001) 168.
[3] A.M. Barnett, D.J. Bassford, J.E. Lees, J.S. Ng, C.H. Tan, J.P.R. David, Nucl. Instrum. Methods. Phys. Res. Sect. A 621 (2010) 453.
[4] G. Bertuccio, S. Caccia, D. Puglisi, D. Macera, Nucl. Instrum. Methods. Phys. Res. Sect. A 652 (2011) 193.
[5] S. Butera, G. Lioliou, A.B. Krysa, A.M. Barnett, J. Appl. Phys. 120 (2016) 024502.
[6] A. Auckloo, J.S. Cheong, X. Meng, C.H. Tan, J.S. Ng, A.B. Krysa, R.C. Tozer, J.P.R. David, J. Inst. 11 (2016) P03021.
[7] J.S. Cheong, J.S.L. Ong, J.S. Ng, A.B. Krysa, J.P.R. David, IEEE J. Sel. Top. Quantum Electron. 20 (2014) 142.
[8] J.S.L. Ong, J.S. Ng, A.B. Krysa, J.P.R. David, IEEE Electron Device Lett. 32 (2011) 1528.
[9] C. Kittel, Introduction to Solid State Physics, eighth ed., John Willey & Sons, New Jersey, 2005.
[10] D.T. Cromer, D. Liberman, J. Chem. Phys. 53 (1970) 1891.
[11] R. Jenkins, R.W. Gould, D. Gedcke, Quantitative X-Ray Spectrometry, second ed., CRC Press, New York, 1995.
[12] U.V. Desnica, Prog. Cryst. Growth Charact. Mater. 36 (1998) 291.
[13] K. Kishino, A. Kikuchi, Y. Kaneko, I. Nomura, Appl. Phys. Lett. 58 (1991) 1822.
[14] R.V. Chelakara, M.R. Islam, J.G. Neff, K.G. Fertitta, A.L. Holmes, F.J. Ciuba, R.D. Dupuis, T.A. Richard, Jr.N. Holonyak, K.C. Hsieh, Appl. Phys. Lett. 65 (1994) 854.
[15] P.M. Smowton, J. Lutti, G.M. Lewis, A.B. Krysa, J.S. Roberts, P.A. Houston, IEEE J. Sel. Top. Quantum Electron. 11 (2005) 1035.
[16] C.N. Atkins, A.B. Krysa, D.G. Revin, K. Kennedy, J.P. Commin, J.W. Cockburn, Electron. Lett. 47 (2011) 1193.
[17] K.A. Bertness, S.R. Kurtz, D.J. Friedman, A.E. Kibbler, C. Kramer, J.M. Olson, Appl. Phys. Lett. 65 (1994) 989.
[18] C. Li, Y.G. Zhang, Y. Gu, K. Wang, A.Z. Li, H. Li, X.M. Shao, J.X. Fang, J. Cryst. Growth 323 (2011) 501.
[19] G.W. Fraser, X-Ray Detectors in Astronomy, Cambridge University Press, Cambridge, 1989.
[20] G. Bertuccio, D. Maiocchi, J. Appl. Phys. 92 (2002) 1248.
[21] G. Bertuccio, R. Casiraghi, IEEE Trans. Nucl. Sci. 50 (2003) 175.
[22] A.M. Barnett, J.E. Lee, D.J. Bassford, J.S. Ng, J. Inst. 7 (2012) P06016.
[23] M.D.C. Whitaker, S. Butera, G. Lioliou, A.M. Barnett, J. Appl. Phys. 122 (2017) 034501.
[24] T. Suzuki, A. Gomyo, S. Iijima, J. Cryst. Growth 99 (1990) 60.
[25] G. Lioliou, A.M. Barnett, Nucl. Instrum. Methods. Phys. Res. Sect. A 836 (2016) 37.
[26] G. Bertuccio, P. Rehak, D. Xi, Nucl. Instrum. Methods. Phys. Res. Sect. B 326 (1993) 71.
[27] U. Shotzig, Appl. Radiat. Isot. 53 (2000) 469.
[28] G. Bertuccio, Nucl. Instrum. Methods. Phys. Res. Sect. A 546 (2005) 232.
[29] A.M. Barnett, J.E. Lee, D.J. Bassford, Appl. Phys. Lett. 102 (2013) 181119.
[30] G. Bertuccio, A. Pullia, J. Lauter, A. Forster, H. Luth, IEEE Trans. Nucl. Sci. 44 (1997) 1.
[31] R.H. Pehl, F.S. Goulding, D.A. Landis, M. Leinzlinger, Nucl. Instrum. Methods. 59 (1968) 45.
[32] A. Rothwarf, J. Appl. Phys. 44 (1973) 752.
[33] R.C. Alig, S. Bloom, Phys. Rev. Lett. 35 (1975) 1522.
[34] C.A. Klein, J. Appl. Phys. 39 (1968) 2029.
[35] A. Owens, A. Peacock, Nucl. Instrum. Methods. Sect. A 531 (2004) 18.